Journal of Photochemistry and Photobiology A: Chemistry 205 (2009) 28–33

Contents lists available at ScienceDirect

Journal of Photochemistry and Photobiology A: Chemistry

journal homepage: www.elsevier.com/locate/jphotochem

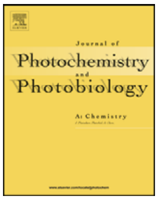

Photocatalytic oxidation of nitrogen monoxide using TiO_2 thin films under continuous UV light illumination

Yoshihisa Ohko*, Yuri Nakamura, Nobuaki Negishi, Sadao Matsuzawa, Koji Takeuchi

Research Institute for Environmental Management Technology, National Institute of Advanced Industrial Science and Technology (AIST), 16-1, Onogawa, Tsukuba, Ibaraki 305-8569, Japan

ARTICLE INFO

Article history:
Received 17 December 2008
Received in revised form 4 March 2009
Accepted 10 April 2009
Available online 18 April 2009

Keywords:
TiO_2 photocatalysis
NO
HNO_3
NO_3
Surface diffusion
Deactivation

ABSTRACT

An apparent deactivating behavior of TiO_2 photocatalysts in NO (1 ppm) oxidation in air was examined using TiO_2 nanoparticulate thin films (0.5–1.4 μm thick) under continuous UV light illumination (1 mW cm^{-2}). The rate of NO oxidation decreased with HNO_3 accumulation on the TiO_2 surface. At the final steady state, the rate of NO oxidation was one-third of the initial one, and NO_2 was released into air at the equivalent rate. The amount of HNO_3 trapped on the TiO_2 film was increased and finally saturated, at which the largest amount of HNO_3 was proportional to the thickness of the film, and then the maximum density of HNO_3 on the TiO_2 surface was estimated to be ∼0.5 molecule nm^{-2}. The value was much smaller than the previously reported one in the NO_2 oxidation (∼2 molecule nm^{-2}). The discrepancy is explained by the consumption of HNO_3 during the photocatalytic reaction, thus HNO_3 reacts with NO and produces NO_2 on the TiO_2 surface under UV light illumination. On the basis of the results, we concluded that the maximum surface density of HNO_3 on TiO_2 in the NO oxidation is determined by the balance between the accumulation amount and the consumption amount of HNO_3 on the TiO_2 surface.

1. Introduction

Titanium dioxide (TiO_2) exhibits photocatalytic reactions on the surface under UV light illumination [1–4]. Electron-hole pairs are generated in TiO_2 when UV light photons are absorbed by TiO_2. The photo-generated holes have strong oxidizing power (∼3.0 V vs SHE) with which most pollutants in air and water can be completely decomposed and mineralized. Removal of nitrogen oxides (NO_x) has been intensively studied by using TiO_2 photocatalysts, and it is recognized as one of the promising applications of TiO_2 photocatalysts [5–10]. NO_x in air is oxidized to nitric acid (HNO_3) by TiO_2 photocatalysis, and the produced HNO_3 molecules are trapped on the TiO_2 photocatalysts [5] due to the high solubility of HNO_3 into water adsorbed on the TiO_2 surface. However, the trapped HNO_3 serves as a physical barrier, decreasing the photocatalytic activity of TiO_2. The long-time stability of TiO_2 photocatalysts is very important to know for the practical use. However, how the reaction rate changes due to the HNO_3 accumulation on the TiO_2 surface has not been investigated in a systematic way.

NO is known to be contained a lot in exhaust gas from automobiles and boilers, and causes various environmental problems. Therefore, NO has been used as the reactant in most cases in the study of NO_x removal. However, the reaction pathways of NO_x gas, including via photocatalytic reactions, are very complicated and inscrutable. For example, NO_2 is easily produced and released into air on the way to the production of HNO_3 [5]. NO_2 is likely to be reduced to NO by photolysis ($NO_2 + h\nu \rightarrow NO + O$) [11]. Besides, NO can react with NO_2 without TiO_2 photocatalysis ($NO + NO_2 + H_2O \rightarrow 2HNO_2$) [11]. Nakamura et al. proved that the photocatalytic oxidation of NO proceeds consecutively as $NO \rightarrow NO_2^- \rightarrow NO_3^-$ on TiO_2 powders by *in situ* Fourier transform infrared (FTIR) spectroscopy [6]. However, the authors did not observe the concentration changes of NO and NO_2 during the reaction; thus, the deactivating behavior of the TiO_2 photocatalyst was not shown.

To understand the detailed reaction dynamics on TiO_2 photocatalysts in NO oxidation, we approach the issue by the original means to use TiO_2 thin films (∼1 μm) consisting of only nanoparticles of TiO_2 (anatase, 20 nm diameter) having the same surface roughness in a typical flow-type reactor for photocatalysis. By using such nanoporous TiO_2 thin films, all of the HNO_3 trapped on the TiO_2 surface can be extracted with water, the amount of the HNO_3 becomes sufficiently larger to detect by ion chromatography (IC), and we can ignore the influence of the surface roughness of these films on the NO_x oxidation rate. Then, by analyzing the film thickness dependency on the initial reaction rate, the deactivation rate, and the accumulated amount of HNO_3, the following information is obtained: the reaction zone on top of the film, the surface diffusion of the produced HNO_3, and the maximum density of HNO_3 accumulated on the TiO_2 surface, respectively. So far, most researchers have

---

* Corresponding author.
E-mail address: y-ohko@aist.go.jp (Y. Ohko).

1010-6030/$ – see front matter © 2009 Elsevier B.V. All rights reserved.
doi:10.1016/j.jphotochem.2009.04.005

tested to introduce their developed photocatalysts to the outdoor air purification along heavy traffic roads, in which a huge volume of polluted air exists. Since TiO_2 photocatalysis is a heterogeneous reaction on the TiO_2 surface, a large quantity of powdery samples with larger surface areas was preferably used in the experiments [5–10]. However, such samples make it very difficult to analyze how the reaction dynamics are complex on the TiO_2 surface.

We have previously reported on the nitrogen dioxide (NO_2, 1 ppm) oxidation in air by using TiO_2 nanoparticulate thin films (0.5–1.5 μm thick) coated on glass plates under continuous UV light illumination over 10 h [12]. The deactivating behavior of the TiO_2 films was indicative that the produced HNO_3, inhibiting the reaction as a physical barrier, is able to diffuse on the TiO_2 surface, and finally distributes homogeneously on the whole film. Then, we could evaluate the reaction zone on top of the TiO_2 film (less than 500 nm) and the maximum density of HNO_3 on the TiO_2 surface (∼2 molecules nm^{-2}). Besides, the photocatalytic activity was found to be remained ∼8% of the initial one at the final steady state. These showed that our original approach is novel and useful for clarifying some important factors in photocatalytic NO_x oxidation.

However, we cannot predict all in the NO oxidation by analogy of the previous results of the NO_2 oxidation. Even though the produced HNO_3 will be accumulated in the TiO_2 films, the reaction zone of the TiO_2 films, the deactivating rate of the TiO_2 films and the surface density of HNO_3, etc. are unknown. If we find some difference in the physicochemical factors, it triggers reconsideration of the NO_x reaction mechanism. Thus, we must investigate anew the deactivating behavior of TiO_2 thin films in NO oxidation by monitoring the changes in NO, NO_2, HNO_2/NO_2^- and HNO_3/NO_3^- under continuous UV light illumination. As a result, we have verified that the maximum surface density of HNO_3 on the TiO_2 surface in the NO oxidation becomes much smaller than that in the NO_2 oxidation. This overturns the common belief that HNO_3 is the final stable product in the TiO_2 photocatalytic oxidation of NO_x. Consequently, we were able to demonstrate that the HNO_3 pre-deposited on the TiO_2 film reacts with NO gas in air and produces NO_2 gas induced by photocatalysis. The information is necessary for comprehending the reaction dynamics on the TiO_2 surface in NO oxidation and for designing more advanced photocatalytic systems for NO purification.

In the present study, we have conducted the experiments of NO (1 ppm) oxidation in air using TiO_2 nanoparticulate thin films (0.5–1.4 μm thick) in a flow-type reactor under continuous UV light illumination (1 mW cm^{-2}) [12]. We have observed changes in the amount of NO, NO_2, HNO_2/NO_2^- and HNO_3/NO_3^- (a NO–NO_x analyzer for NO and NO_2, ion chromatography for HNO_2/NO_2^- and HNO_3/NO_3^-, respectively). From the time dependency and the thickness-dependency on these parameters, the surface density of HNO_3 at the final steady state was estimated. Comparing with the previous data in the NO_2 oxidation, [12] we have speculated the photocatalytic reaction of HNO_3 and experimentally demonstrated the reaction for the first time.

2. Experimental

A TiO_2 thin film was prepared on a Pyrex glass plate (5 × 10 cm^2) by a conventional spin coating process, using a TiO_2 anatase aqueous sol (Ishihara Sangyo Kaisha Ltd., STS-21, 20 nm particle diameter) [12]. The second and the third coatings were applied in the same manner over the first coating. The thickness of the TiO_2 film increased approximately 0.5 μm per one-time coating [12]. Three types of the TiO_2 film were used in the experiment, whose thickness and weight were (1) 0.5 μm and 4.6 mg, (2) 0.9 μm and 8.8 mg, and (3) 1.4 μm and 12.9 mg, respectively. The mean porosity of the TiO_2 films was 49 ± 5%, and the mean roughness of the TiO_2 film surfaces was almost constant, ∼26.5 nm [12]. The TiO_2-coated glass plates were immersed in deionized water for more than 24 h under UV light illumination with a black fluorescent lamp (Toshiba Co., FL10BLB-A; wavelength, 300–400 nm; UV intensity, 2 mW cm^{-2}) in order to remove residual organic matter and water-soluble inorganic contamination from the TiO_2 surface, as evidenced by ion chromatography (IC; Tosoh, IC-2001).

All of the photocatalytic reactions of NO were carried out at room temperature (298 K). The reaction gas was prepared from a NO–N_2 gas mixture (Takachiho Chemicals Co., ∼100 ppm, ∼20 mL min^{-1}) as well as purified dry air (1 L min^{-1}) and purified wet air (1 L min^{-1}, created through a humidifier), attained by using thermal mass-flow controllers. The relative humidity (RH) of the reaction gas was adjusted to 50% and the NO concentration was kept at 1 ppm. A typical flow-type reactor for photocatalysis was used, in which the layer of the reaction gas over the sample plate was 5 mm thick, and the reaction gas was passed through the reactor at a flow-rate of 2 L min^{-1} (laminar flow). The UV light source was a black fluorescent lamp, set over the photoreactor. NO_x (NO and NO_2) in the gas phase was monitored with a chemiluminescent NO–NO_x analyzer (Monitor Labs Inc., Model 9841A). The reaction products remaining on the TiO_2 were extracted by immersing the sample into deionized water (10 mL) for 30 min, and measured using IC (column, TSKgel SuperIC-AZ; eluent, 1.9 mM $NaHCO_3$ and 3.2 mM Na_2CO_3). All of the data were collected using the same TiO_2 thin films in order to avoid variations in activity caused by the difference of the surface area and thickness.

3. Results and discussion

3.1. Photocatalytic oxidation of NO

Fig. 1(a) shows typical experimental data for the concentration changes of NO, NO_2, and NO_x (the sum of NO and NO_2) as a function of UV light illumination time in the NO oxidation by using the thinnest TiO_2 film (0.5 μm). Before UV light illumination, we adjusted the initial NO concentration to 1 ppm (time period (i)) and investigated the amount of NO adsorbed on the TiO_2 film by passing the reaction gas through the reactor in the dark for 10 min (time period (ii)). However, adsorption of NO on the TiO_2 film was negligible since the NO concentration did not change during the time period (ii). When UV light illumination was started, the NO concentration in the outlet gas went down steeply to ∼0.45 ppm. Then, it was immediately increased to ∼0.8 ppm and remained constant. Corresponding to the concentration change of NO, the NO_2 concentration increased steeply to ∼0.3 ppm and decreased to ∼0.2 ppm, keeping in mind that the time for the positive peak of NO_2 concentration is not exactly the same as the time for the negative peak of NO concentration, usually ∼1 min later. The sequence of reactions that produce NO_2 and HNO_3/NO_3^- is considered as follows [13–17]:

$$h\nu \rightarrow h^+ + e^- \tag{1}$$

$$h^+ + O_s^{2-} \rightarrow O_s^- \tag{2}$$

$$NO + h^+ + H_2O_{ads} \rightarrow HNO_2 + H^+ \tag{3}$$

$$\begin{aligned} NO + O_s^- + H_2O_{ads} &\rightarrow HNO_2 + V[O_s^{2-}] + OH^-_{ads} \\ &\rightarrow HNO_2 + O_s^{2-} + H^+ \end{aligned} \tag{4}$$

$$HNO_2 + h^+ \rightarrow NO_2 + H^+ \tag{5}$$

$$HNO_2 + O_s^- \rightarrow NO_2 + O_s^{2-} + H^+ \tag{6}$$

$$HNO_2 + O_s^- \rightarrow HNO_3^- + V[O_s^{2-}] \tag{7.1}$$

$$V[O_s^{2-}] + OH^-_{ads} \rightarrow O_s^{2-} + H^+ \tag{7.2}$$

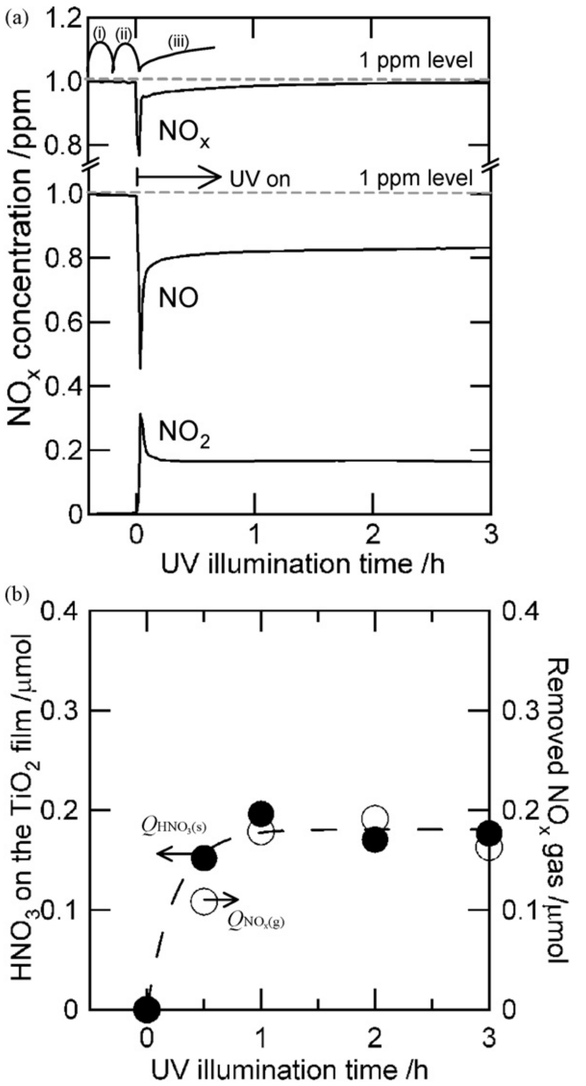

Fig. 1. (a) Concentrations of NO, NO_2, and NO_x (= NO + NO_2) as a function of UV illumination time in the photocatalytic oxidation of NO (thickness of the TiO_2 film, 0.5 μm; UV intensity, 1 mW cm^{-2}; initial NO concentration, 1 ppm; time period (i): the reaction gas did not pass through the reactor for measuring the initial concentration of NO; time period (ii): the reaction gas passed through the reactor in the dark for measuring the adsorption of NO on the TiO_2 film; time period (iii): the sample was illuminated with UV light for conducting the photocatalytic oxidation of NO). (b) The amount of HNO_3 recovered from the TiO_2 film ($Q_{HNO_3(s)}$) (●) and that of NO_x removed from air ($Q_{NO_x(g)}$) (○) as a function of UV illumination time (each plot was acquired by repeating a separate experiment in which UV illumination stopped at a given time). The broken line fit the plots of $Q_{HNO_3(s)}$ in an exponential approximation as eye-guide.

$$HNO_3{}^{-} + O_s{}^{-} \rightarrow HNO_3 + O_s{}^{2-} \tag{7.3}$$

$$NO_2 + h^{+} + H_2O_{ads} \rightarrow HNO_3 + H^{+} \tag{8}$$

$$\begin{aligned} NO_2 + O_s{}^{-} + H_2O_{ads} &\rightarrow HNO_3 + V[O_s{}^{2-}] + OH^{-}{}_{ads} \\ &\rightarrow HNO_3 + O_s{}^{2-} + H^{+} \end{aligned} \tag{9}$$

$$NO_2 + O_s{}^{-} \rightarrow NO_3{}^{-} + V[O_s{}^{2-}] \tag{10.1}$$

$$V[O_s{}^{2-}] + OH^{-}{}_{ads} \rightarrow O_s{}^{2-} + H^{+} \tag{10.2}$$

where $O_s{}^{2-}$ represents terminal (bridging) oxygen ions and $V[O_s{}^{2-}]$ are bridging oxygen vacancies. The photo-excited electrons (e^-) will be captured by oxygen molecules (O_2) in air, and then produced superoxide radicals ($O_2{}^{\bullet -}$) and hydroperoxyl radicals ($HO_2{}^{\bullet}$) also contribute to the NO oxidation, e.g., NO + $HO_2{}^{\bullet} \rightarrow HNO_3$, etc.

The amount of HNO_3, produced and trapped on the TiO_2 surface, increased with UV light irradiation time, and saturated at ~0.2 μmol after 1 h (Fig. 1(b)). In this experiment, only $NO_3{}^{-}$ was detected by IC. The time dependency of the concentration of NO is explained as follows: HNO_3 is rapidly produced and accumulated on top of the TiO_2 film surface, and therefore inhibiting the photocatalytic reactions as a physical barrier.

The apparent quantum yield (QY) was estimated using the following equations:

$$QY = \frac{\text{number of removed NO molecules}}{\text{number of incident photons}} \tag{11}$$

then, the QY value just after UV light illumination at which NO decreased the most was approximately ~0.5%. The value was higher than that (0.3%) in the NO_2 oxidation [12].

To consider the nitrogen mass balance during the photocatalytic oxidation of NO, the amount of HNO_3 recovered from the TiO_2 film ($Q_{HNO_3(s)}$) was compared with the amount of NO_x (NO and NO_2) removed from air ($Q_{NO_x(g)}$). $Q_{NO_x(g)}$ was calculated as follows:

$$Q_{NO_x(g)} = Q_{NO(g)} - Q_{NO_2(g)} \tag{12}$$

$$= \left\{ \int ([NO]_{initial} - [NO]_{UV})dt - \int ([NO_2]_{UV} - [NO_2]_{initial})dt \right\} \times \left(\frac{V}{22.4} \right) \tag{13}$$

where $Q_{NO(g)}$ is the amount of NO removed from air (μmol), $Q_{NO_2(g)}$ is the amount of NO_2 released into air (μmol), $[NO]_{initial}$ is the concentration of NO in the inlet gas (ppm), $[NO]_{UV}$ is the concentration of NO in the outlet gas under UV light illumination (ppm), $[NO_2]_{initial}$ is the concentration of NO_2 in the inlet gas (ppm), $[NO_2]_{UV}$ is the concentration of NO_2 in the outlet gas under UV light illumination (ppm), and V is the flow rate of the reaction gas (L min^{-1}) under standard conditions (0 °C and 1.013 hPa). As shown in Fig. 1(b), $Q_{NO_x(g)}$ agreed closely with $Q_{HNO_3(s)}$ during 3 h of UV light illumination.

Even at the final steady state, NO was oxidized at one-third of the initial oxidation rate. Although the NO oxidation rate was not so decreased, the production of HNO_3 was completely stopped. The mechanism cannot be explained only by assuming that the HNO_3 serves as an inert physical barrier. The problem will be discussed later (see below).

3.2. Film thickness dependence of the reaction

Fig. 2 (a)–(c) shows the concentration changes of NO, NO_2, and NO_x, in which the UV illumination time period was 0.5 h and 10 h, and the change in $Q_{HNO_3(s)}$ as a function of UV light illumination time in the photocatalytic oxidation of NO using the TiO_2 films with different thickness (0.5 μm, 0.9 μm, and 1.4 μm). For comparison, data of the three samples are overlaid. Let us analyze the data in five terms: (A) the initial oxidation rate, (B) the deactivation behavior, (C) $Q_{HNO_3(s)}$, (D) the final steady state, and (E) the nitrogen mass balance. Concerning (A), the initial oxidation rate of NO increased slowly with increasing thickness of TiO_2 films. This indicates that the reaction zone of the TiO_2 film for the NO oxidation was not limited within 0.5 μm thick (Fig. 2(a)). Concerning (B), for example, the slope of the NO concentration change while upturning to the initial one (1 ppm) became smaller with increasing thickness of TiO_2 films. The order of deactivation behavior of the TiO_2 film coincided to that obtained in the NO_2 oxidation as reported previously [12]. As for (C), $Q_{HNO_3(s)}$ was increased with increasing the film thickness, and reached the maximum values for each the TiO_2

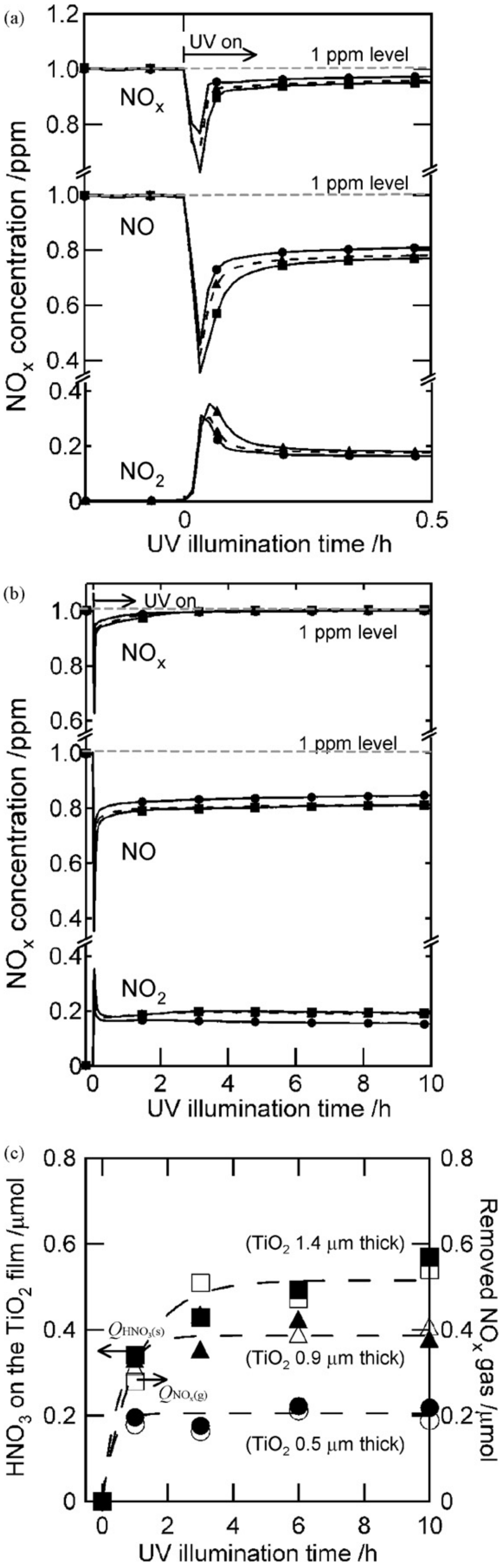

Fig. 2. Concentrations of NO, NO_2, and NO_x ((a) a short-time view, (b) a long-time view), and (c) $Q_{HNO_3(s)}$ as a function of UV illumination time in the NO oxidation using the TiO_2 films with different thickness (thickness of the TiO_2 film:(●) 0.5 μm, (▲) 0.9 μm, (■) 1.4 μm; UV intensity, 1 mW cm^{-2}; initial NO concentration, 1 ppm). As for (c), each plot was acquired in the same manner as Fig. 1(b). $Q_{NO_x(g)}$ was also plotted in (c) with the corresponding open symbols to $Q_{HNO_3(s)}$.

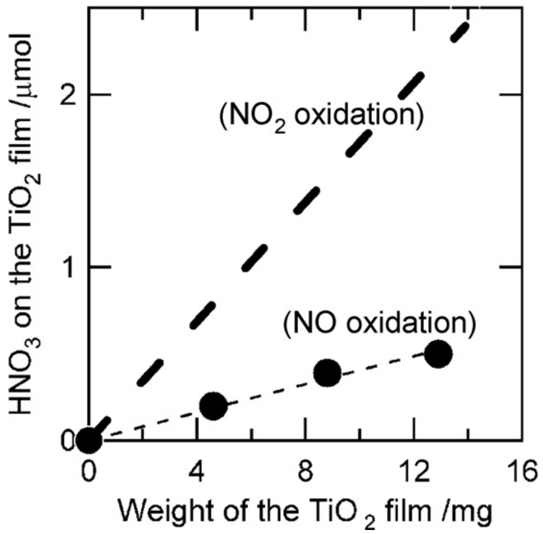

Fig. 3. Dependence of the weight of the TiO_2 film on $Q_{HNO_3(s)}$. The black bold broken line indicates the relationship in the case of NO_2 oxidation as reported previously [12].

film (Fig. 2(c)). These results are reasonably explained by applying the previously proposed model [12] of diffusion and accumulation of HNO_3 on the TiO_2 surface; the produced HNO_3 quickly diffuses inside of the TiO_2 film, by which the increase of the surface density of HNO_3 is reduced, and therefore the apparent oxidation rate of NO is decreased slower for thicker films. Regarding (D), the NO concentration was ~0.8 ppm, the NO_2 concentration ~0.2 ppm, and the NO_x removal rate negligible for all the TiO_2 films under continuous UV light illumination. Increasing thickness of TiO_2 films slightly increased the oxidation rate of NO at the final steady state. As for (E), the nitrogen mass balance between $Q_{HNO_3(s)}$ and $Q_{NO_x(g)}$ was always kept as shown in Fig. 2(c). This is different from the case of NO_2 oxidation, [12] in which $Q_{NO_x(g)}$ became larger than $Q_{HNO_3(s)}$ with UV light illumination time.

In Fig. 3, the values of $Q_{HNO_3(s)}$ are plotted as a function of TiO_2 film mass. $Q_{HNO_3(s)}$ had a good proportionality to the weight of TiO_2 films. This indicates that the produced HNO_3 finally accumulated homogeneously in the TiO_2 films. The slope of linear regression is 0.04 ± 0.002 μmol of $Q_{HNO_3(s)}$ per 1 mg of TiO_2. The value of specific surface area of the TiO_2 is 50 m^2 g^{-1} [18]. Thus, the maximum density of HNO_3 on the TiO_2 surface is calculated to be ~0.5 molecules nm^{-2}. The occupied area per one HNO_3 molecule was ca. 2 nm^2. The surface density of HNO_3 was found to be only one-fourth of the previous reported one in the NO_2 oxidation (~2 molecules nm^{-2}) [12].

Because HNO_3 was the common final product, and because all the experimental conditions were the same except the starting reactant, the maximum surface density of HNO_3 must be both consistent. However, the difference was significant. This is not explained without considering some unknown reactions on HNO_3 (see below).

3.3. Photocatalytic reaction of HNO_3 with NO

In order to clarify what happens to HNO_3 on the TiO_2 film under continuous UV light illumination, a preliminary experiment was conducted (Fig. 4): a certain amount of HNO_3 was pre-deposited

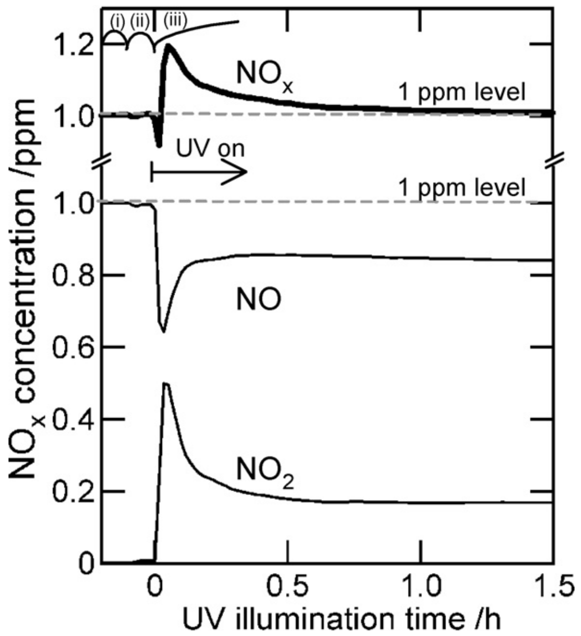

Fig. 4. Concentration changes of NO, NO_2, and NO_x when using the TiO_2 film on which ~0.6 μmol of HNO_3 was pre-deposited.

on the TiO_2 film, and then the sample was exposed to the NO gas (1 ppm in air) as well as illuminated with UV light ($1\,mW\,cm^{-2}$). 0.1 mL of HNO_3 aqueous solution (10 mM) was placed on the TiO_2 film (0.5 μm thick), and dried it in air in the dark (RH, 50%; 25 °C) for 24 h. Then, ~0.6 μmol of HNO_3 remained on the sample. Next, the sample was set in the photoreactor, and the NO gas was let in as usual. Then, the concentrations of both NO and NO_2 were not changed in the dark (time period (ii)). This indicates that HNO_3 on the TiO_2 does not apparently react with dilute NO gas in the dark, though Mochida and Finlayson-Pitts reported the reaction of HNO_3 and gaseous NO (10^3–10^4 ppm) [19]. However, just after the sample was illuminated with UV light, the concentration of NO_x was abruptly increased to ~1.2 ppm, and afterwards gradually decreased to the initial 1 ppm. Just on the UV light illumination, the concentration of NO decreased to ~0.65 ppm, while the concentration of NO_2 was increased to ~0.5 ppm. These values were both higher than the case using the pure TiO_2 film, and the amount of NO_2 released into air was larger than that of NO removed from air during the reaction. Thus, the increase of NO_x concentration over 1 ppm was clearly caused by the pre-deposited HNO_3 on the TiO_2 film, because the amount of NO_x in the outlet gas exceeded that in the inlet gas. Instead of the TiO_2, we used a SiO_2 nanoparticulate film. Then, there were no concentration changes, for both NO and NO_2, in the dark as well as under UV light illumination. The SiO_2 film was prepared from a commercial colloidal SiO_2 solution (Nippon Chemical Industrial Co. Ltd.; particle diameter, 20 nm; film weight, 4 mg) and ~0.5 μmol of HNO_3 was pre-deposited in the same manner as for the TiO_2 film. When using the TiO_2 film without the NO gas, the concentrations of both NO and NO_2 were scarcely changed under UV light illumination. We therefore concluded that HNO_3 reacts with NO owing to the action of TiO_2 photocatalysis. Then, HNO_3 must be oxidized to NO_3, followed by producing NO_2. The possible reactions are considered as follows:

$$HNO_3 + h^+ \rightarrow NO_3 + H^+ \tag{14}$$

$$HNO_3 + O_s{}^- \rightarrow NO_3 + OH^-{}_{ads} \tag{15}$$

$$NO_3{}^- + h^+ \rightarrow NO_3 \tag{16}$$

$$NO_3{}^- + O_s{}^- \rightarrow NO_3 + O_s{}^{2-} \tag{17}$$

$$NO_3 + NO \rightarrow 2NO_2 \tag{18}$$

After 3 h of UV light illumination, only ~0.2 μmol of HNO_3 was recovered from the TiO_2 surface; thus ~0.4 μmol of pre-deposited HNO_3 was lost from the TiO_2 surface. In other words, some of the HNO_3 on the TiO_2 surface was certainly consumed by TiO_2 photocatalytic reaction. The remaining amount of HNO_3 on the TiO_2 surface was equivalent to the maximum accumulated amount of HNO_3 when using the pure TiO_2 film. On the other hand, the amount of NO_x over the initial 1 ppm was calculated to be 0.3 μmol. Thus, the lost HNO_3 was found in the outlet gas as the overproduced NO_2. All of these support the proposed reactions (Eqs. (14–18)).

The formation of NO_3 from the reaction between HNO_3 and free hydroxyl radical ($^{\bullet}OH$) as $HNO_3 + {}^{\bullet}OH \rightarrow NO_3 + H_2O$ has been intensively studied in the atmospheric chemistry [20]. The photocatalytic production of $^{\bullet}OH$ radicals [21] and their participation in the subsequent reactions have been invoked to explain the photocatalytic oxidation of organic compounds. However, recently, Ishibashi et al. estimated the quantum yield of $^{\bullet}OH$ production during TiO_2 photocatalysis to be 7×10^{-5} in aqueous solution, which is much lower than the quantum yield of ordinary photocatalytic reactions ($\sim 10^{-2}$) [22]. In addition, Salvador demonstrated that free $^{\bullet}OH$ radicals cannot be generated via the photooxidation of water molecules or solvated hydroxyl groups with valence band holes of TiO_2 both thermodynamically and kinetically, but may only be generated via the electroreduction of dissolved oxygen with photogenerated conduction band electrons [13]. Thus, $^{\bullet}OH$ radicals are hardly likely to make a major contribution to the result in Fig. 4.

Here, let us consider the problem that has remained unsolved, why the production of HNO_3 was apparently stopped at the final steady state. Certainly, the accumulated HNO_3 molecules did not a little contribute to the decrease of NO oxidation rate as a physical barrier. However, it is much more adequate to consider that the potential of the TiO_2 activity is not reduced at all, but it enables nitrogen oxides, including HNO_3, to be further oxidized even at the final steady state. Therefore, the maximum surface density of HNO_3 in the NO atmosphere will be determined by the balance between the accumulation amount and the consumption amount of HNO_3 on the TiO_2 surface. It could be dependent on several factors, for example, NO concentration, HNO_3 amount, UV light intensity, photocatalytic activity of TiO_2, the film conditions, such as, surface morphologies, grain sizes, film densities, and so on. The detailed kinetic study will be performed in the near future.

4. Conclusions

Photocatalytic oxidation of NO was kinetically studied using TiO_2 nanoparticulate thin films, and we found the following for the first time: (1) The reaction zone on top of the TiO_2 film exists over 500 nm thickness; (2) the rate of NO oxidation soon decreased to one-third of the initial one; (3) at the final steady state, the produced NO_2 was released into air at the equivalent rate of NO oxidation; (4) the amount of HNO_3 on the TiO_2 film was increased and finally saturated, at which the largest amount of HNO_3 was proportional to the thickness of the film, and then the maximum density of HNO_3 on the TiO_2 surface was determined to be ~0.5 molecule nm^{-2}; (5) the nitrogen mass was balanced all the time between the removed NO_x gas and the produced HNO_3; (6) the HNO_3 pre-deposited on the TiO_2 film reacted with NO and produced NO_2 under UV light illumination. From our novel approach and original perspective, the fate of HNO_3 on the TiO_2 in the photocatalytic NO oxidation was revealed for the first time, and it is concluded that the maximum surface density of HNO_3 in the NO oxidation is determined by the balance between the accumulation amount and the consumption amount of HNO_3 on the TiO_2 surface. These findings will be very useful for developing photocatalytic materials for NO_x removal. Since the emission of NO_2 is unfavorable due to its high toxicity and the reaction pathways of nitrogen oxides, including HNO_3, are so complicated that we should apply TiO_2 photocatalysts to NO_x removal with more sufficient care. It is important to remove the produced HNO_3 from the TiO_2 surface before the problematic reaction becomes serious.

Acknowledgements

We express gratitude to Dr. Y. Krockenberger for careful reading the manuscript. This work was supported by Industrial Technology Research Grant Program in 2006 from New Energy and Industrial Technology Development Organization (NEDO) of Japan. We are grateful to Ishihara Sangyo Kaisha Ltd. for supplying the TiO_2 sol.

References

[1] A. Fujishima, K. Honda, Nature 238 (1972) 37.
[2] M. Formenti, H. Courbon, F. Juillet, A. Lissatchenko, J.R. Martin, P. Meriaudeau, S.J. Teichner, J. Vac. Sci. Technol. 9 (1972) 947.
[3] A.G. Agrios, P. Pichat, J. Appl. Electrochem. 35 (2005) 655.
[4] D.T. Tompkins, B.J. Lawnicki, W.A. Zeltner, M.A. Anderson, ASHRAE Trans. 111 (Pt 2) (2005) 60.
[5] T. Ibusuki, K. Takeuchi, J. Mol. Catal. 88 (1994) 93.
[6] I. Nakamura, S. Sugihara, K. Takeuchi, Chem. Lett. (2000) 1276.
[7] H. Ichiura, T. Kitaoka, H. Tanaka, Chemosphere 51 (2003) 855.
[8] Y.M. Lin, Y.H. Tseng, J.H. Huang, C.C. Chao, C.C. Chen, I. Wang, Environ. Sci. Technol. 40 (2006) 1616.
[9] T. Maggos, J.G. Bartzis, P. Leva, D. Kotzias, Appl. Phys. A: Mater. Proc. 89 (2007) 81.
[10] Y. Ishibai, J. Sato, S. Akita, T. Nishikawa, S. Miyagishi, J. Photochem. Photobiol. A: Chem. 188 (2007) 106.
[11] B.J. Finlayson-Pitts, J. James, N. Pitts, Chemistry of the Upper and Lower Atmosphere: Theory, Experiments, and Applications, Academic Press, 1999.
[12] Y. Ohko, Y. Nakamura, A. Fukuda, S. Matsuzawa, K. Takeuchi, J. Phys. Chem. C 112 (2008) 10502.
[13] P. Salvador, J. Phys. Chem. C 111 (2007) 17038.
[14] D. Monllor-Satoca, R. Gomez, M. Gonzalez-Hidalgo, P. Salvador, Catal. Today 129 (2007) 247.
[15] R. Enriquez, A.G. Agrios, P. Pichat, Catal. Today 120 (2007) 196.
[16] J.M. Coronado, J. Soria, Catal. Today 123 (2007) 37.
[17] O.I. Micic, Y.N. Zhang, K.R. Cromack, A.D. Trifunac, M.C. Thurnauer, J. Phys. Chem. 97 (1993) 7277.
[18] http://www.iskweb.co.jp/functional/ISKWEB1-3-photocattop.htm.
[19] M. Mochida, B.J. Finlayson-Pitts, J. Phys. Chem. A 104 (2000) 9705.
[20] R.P. Wayne, I. Barnes, P. Biggs, J.P. Burrows, C.E. Canosamas, J. Hjorth, G. Lebras, G.K. Moortgat, D. Perner, G. Poulet, G. Restelli, H. Sidebottom, Atmos. Environ. 25A (1991) 1.
[21] C.D. Jaeger, A.J. Bard, J. Phys. Chem. 83 (1979) 3146.
[22] K. Ishibashi, A. Fujishima, T. Watanabe, K. Hashimoto, J. Photochem. Photobiol. A: Chem. 134 (2000) 139.